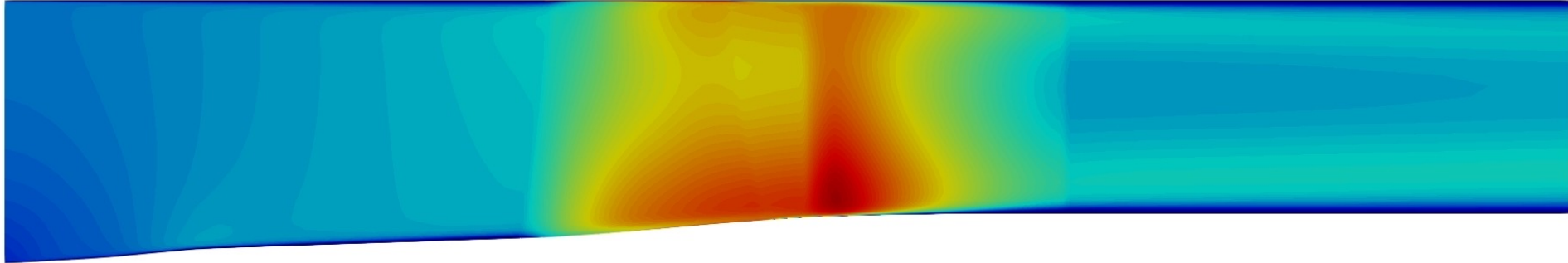


Geometric uncertainties in through-flow models



Arnaud Budo⁽¹⁾

Octobre 2018 → Octobre 2023

Vincent E. Terrapon⁽¹⁾, Maarten Arnst⁽¹⁾

Sophie Mouriaux⁽²⁾, Jules Bartholet⁽³⁾

Journée des doctorants HAIDA 2021



Context

Geometrical variability of aerodynamic parts
of low-pressure compressors



[SAB]

Technical and economic
performances

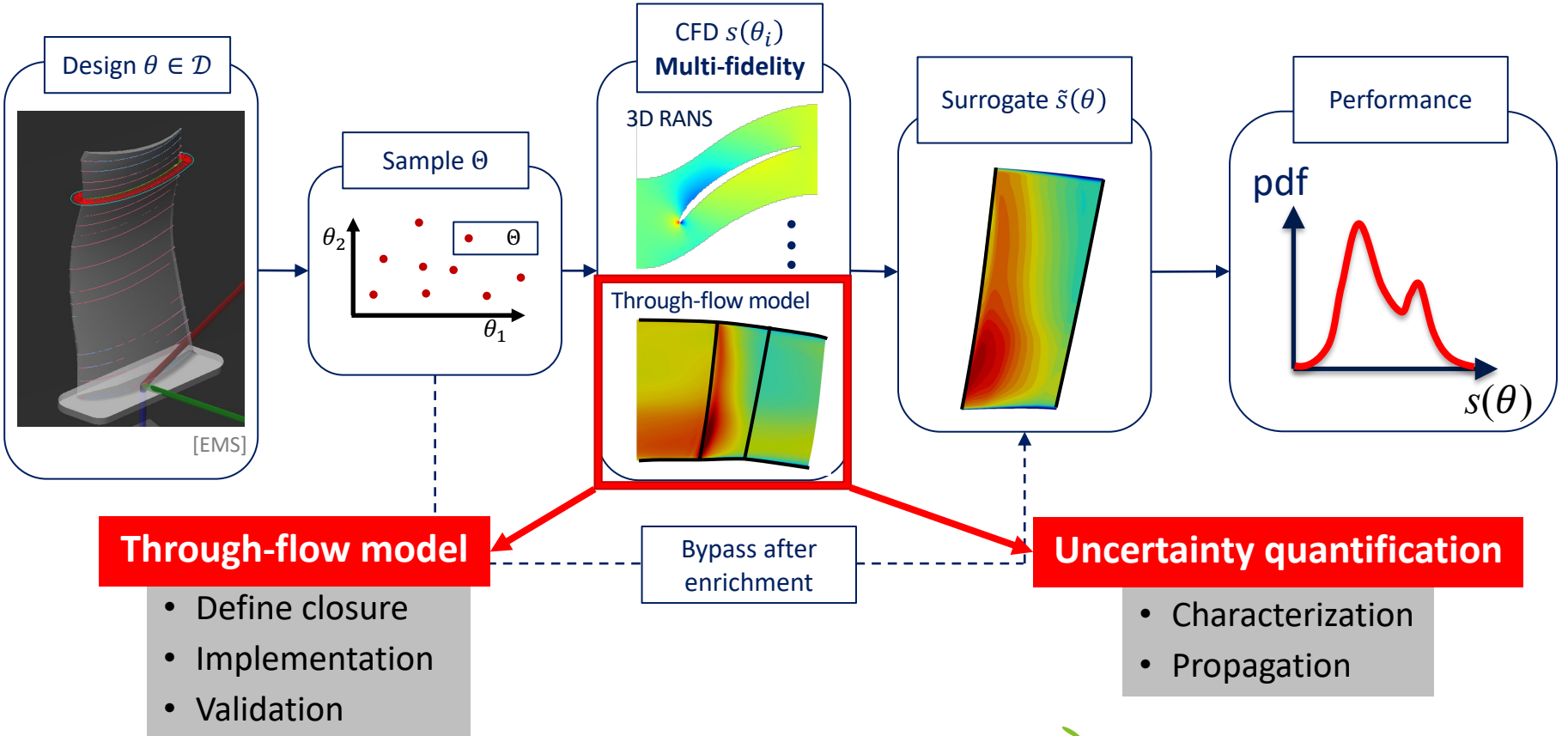
Manufacturing tolerances?

- Rigorous/robust methodology
- Choice of manufacturing process
- Simplify the treatment of poorly made parts

Decrease the
overall cost

Methodology

Characterization
Propagation
Qualification



Outline

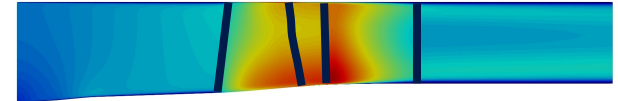
1

Viscous
through-flow model

$$\frac{\partial U}{\partial t} + \frac{\partial(F-F_v)}{\partial x} + \frac{\partial(G-G_v)}{\partial r} = S$$

2

Application to the CME2
compressor stage



3

Application to an axial LP
compressor



4

Future work



[SAB]

Outline

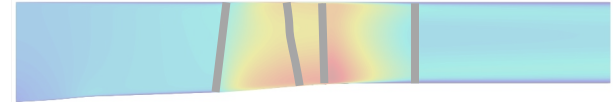
1

**Viscous
through-flow model**

$$\frac{\partial U}{\partial t} + \frac{\partial(F-F_v)}{\partial x} + \frac{\partial(G-G_v)}{\partial r} = S$$

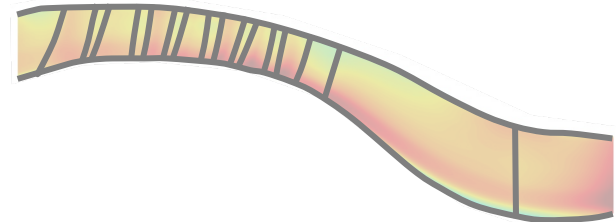
2

**Application to the CME2
compressor stage**



3

**Application to an axial LP
compressor**



4

Future work



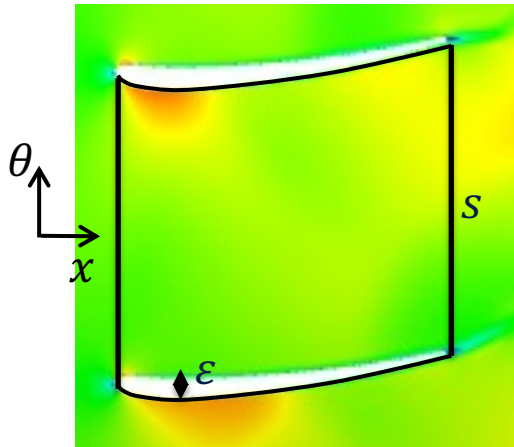
[SAB]

Viscous through-flow model

Circumferential averaged Navier-Stokes equations:



Conservative variables



$$\frac{\partial U}{\partial t} + \frac{1}{b} \frac{\partial b (F - F_v)}{\partial x} + \frac{1}{b} \frac{\partial b (G - G_v)}{\partial r} = \mathbf{S}$$

$\overbrace{\quad}^{x\text{-fluxes}}$ $\overbrace{\quad}^{r\text{-fluxes}}$

Blockage factor

$$b = 1 - \frac{\varepsilon(x)}{s}$$

- Inviscid blade force
- Viscous blade force
- Reynolds stress
- Axisymmetric source terms

Non-intrusive formulation for elsA:

[Onera]

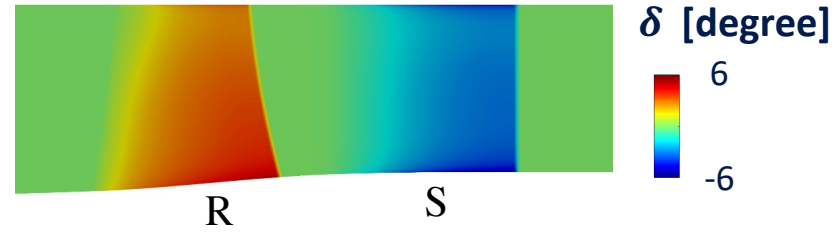
$$\frac{\partial U}{\partial t} + \frac{\partial (F - F_v)}{\partial x} + \frac{\partial (G - G_v)}{\partial r} = \mathbf{S} + \frac{(\cancel{F}_v - F)}{b} \frac{\partial b}{\partial x} + \frac{(\cancel{G}_v - G)}{b} \frac{\partial b}{\partial r}$$

Blockage factor terms

ASTEC: correlations for δ and ω

Deviation angle δ (inviscid blade force)

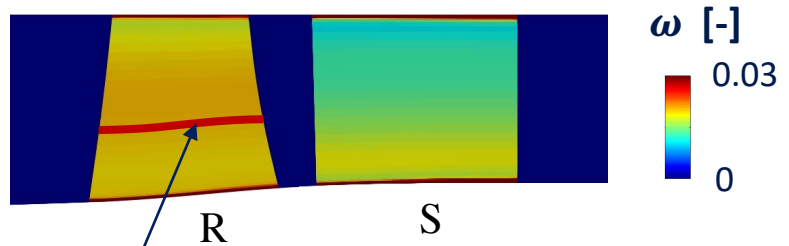
- From cascade experiments (Lieblein)
- Linear variation with incidence around design conditions
- $\delta = \delta_{TE} \frac{\kappa_{LE} - \kappa}{\kappa_{LE} - \kappa_{TE}}$ ← Blade angle



- NACA65
- C4
- Double circular arc

Loss coefficient ω (viscous blade force)

- From cascade experiments (Lieblein)
- Design + off-design parts



Profile loss only

Constant over streamline (0D)

Outline

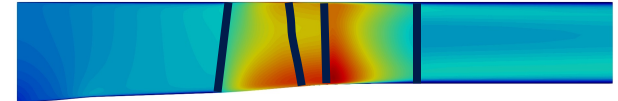
1

Viscous
through-flow model

$$\frac{\partial U}{\partial t} + \frac{\partial(F-F_v)}{\partial x} + \frac{\partial(G-G_v)}{\partial r} = S$$

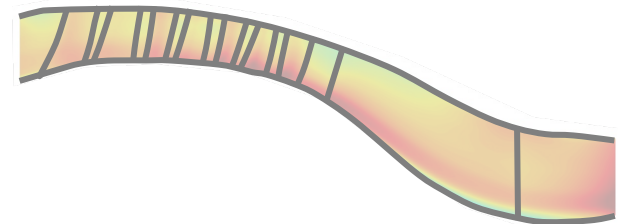
2

Application to the CME2
compressor stage



3

Application to an axial LP
compressor



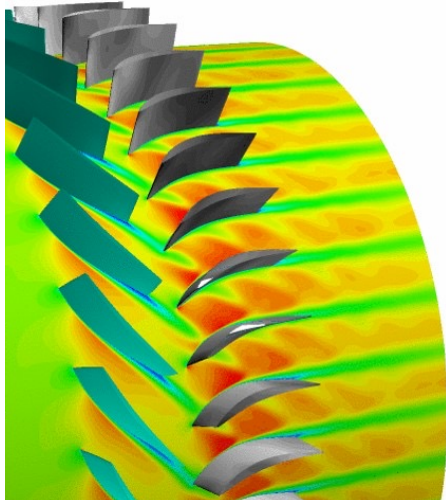
4

Future work



[SAB]

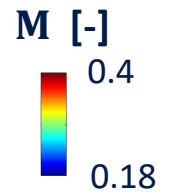
CME2: Overview



[Moreau 2019]

- Research compressor designed by Safran Aircraft Engines
- Low speed flow
- NACA65A012 blades
- Correlations calibrated at these conditions

Mach number



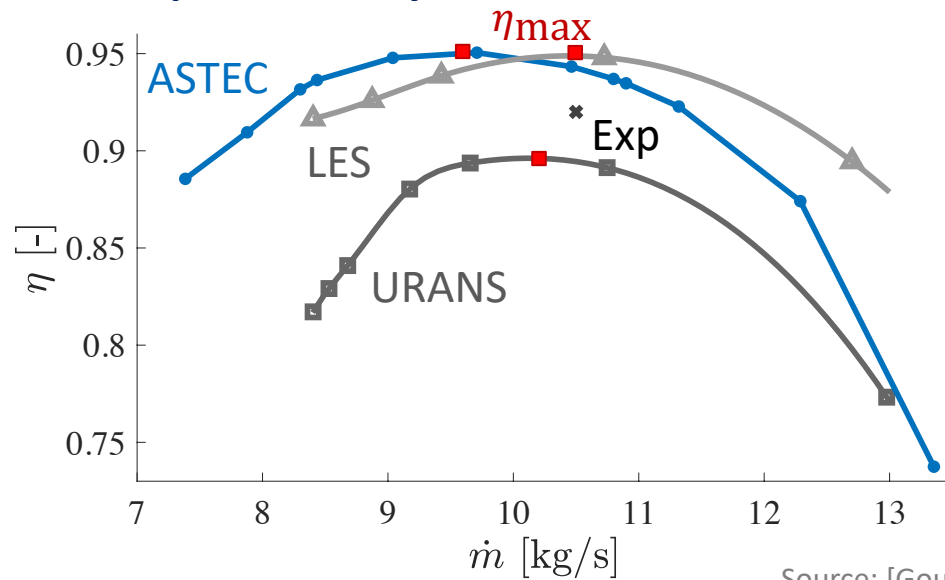
R

S

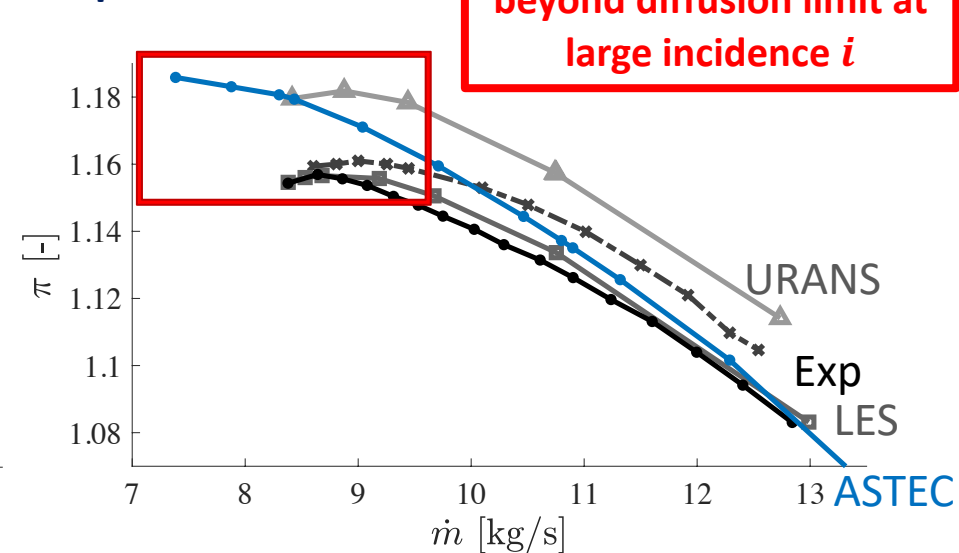
CME2: results

- Globally good agreement
- Relative difference lower than LES-URANS discrepancy
- ASTEC maximum peak efficiency close to LES prediction
- Slight shift of mass-flow rate
- Discrepancies near stall

Isentropic efficiency



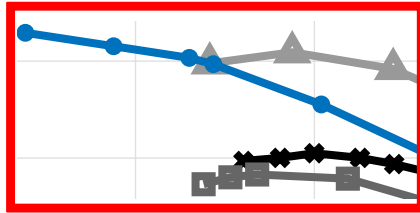
Total pressure ratio



Source: [Gourdain 2015]

CME2: Diffusion limit

Total pressure ratio

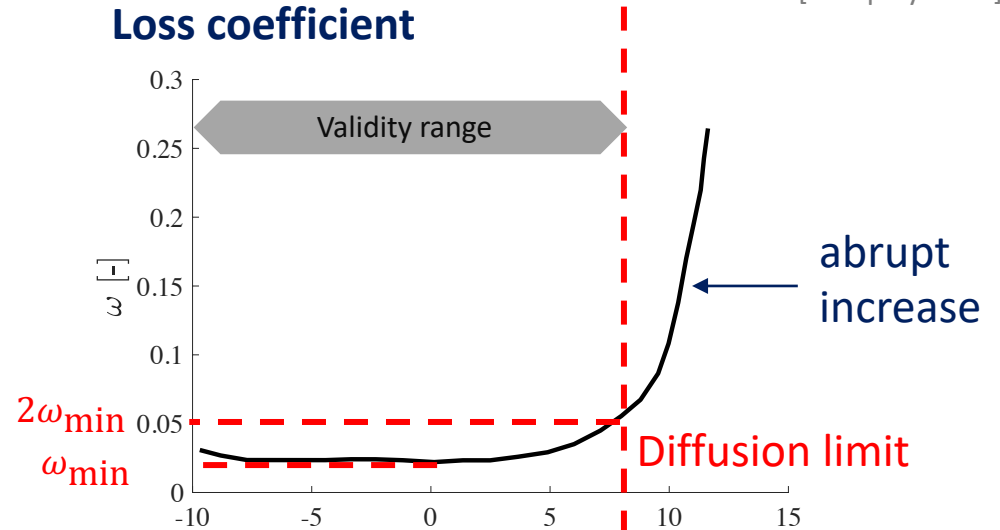


**Assumptions of loss correlations
not valid beyond diffusion limit
at large incidence i**

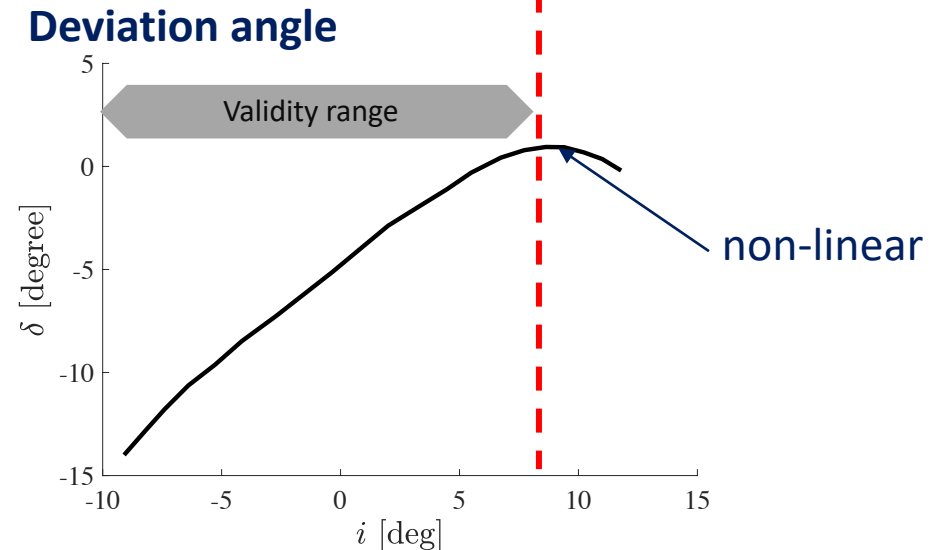
Measurements of C4-series cascade ($M = 0.4$)

[Cumpsty 1989]

Loss coefficient



Deviation angle



Outline

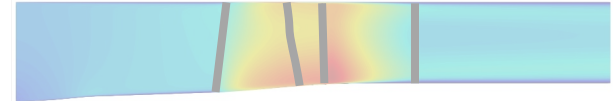
1

Viscous
through-flow model

$$\frac{\partial U}{\partial t} + \frac{\partial(F-F_v)}{\partial x} + \frac{\partial(G-G_v)}{\partial r} = S$$

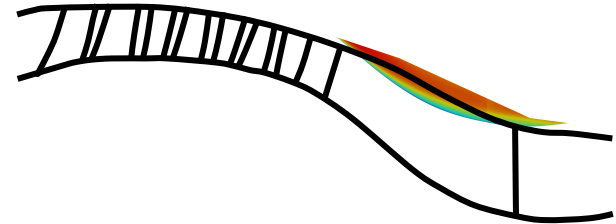
2

Application to the CME2
compressor stage



3

Application to an axial LP
compressor



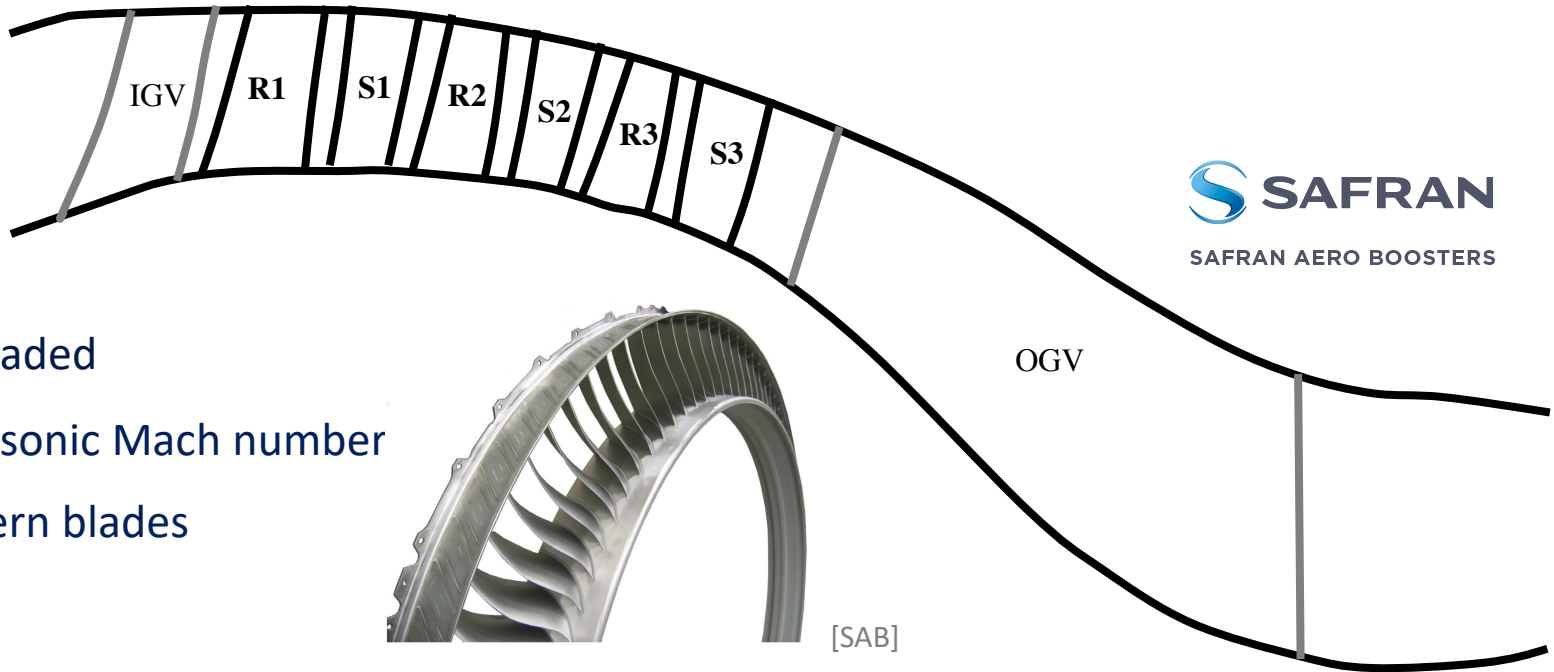
4

Future work

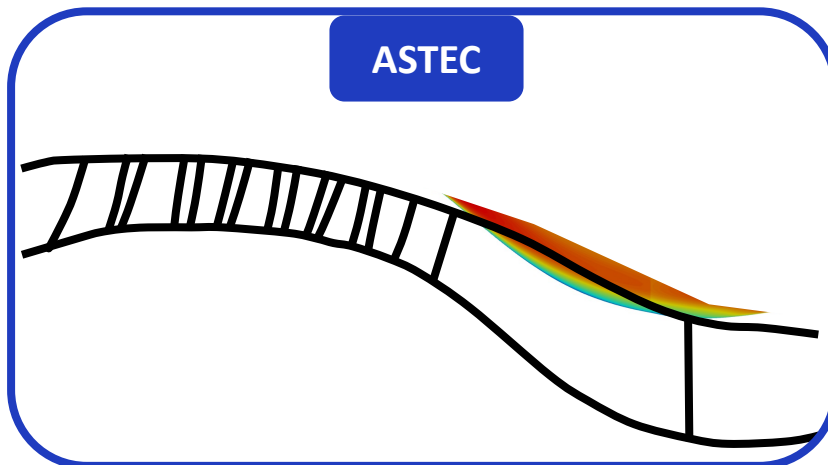


[SAB]

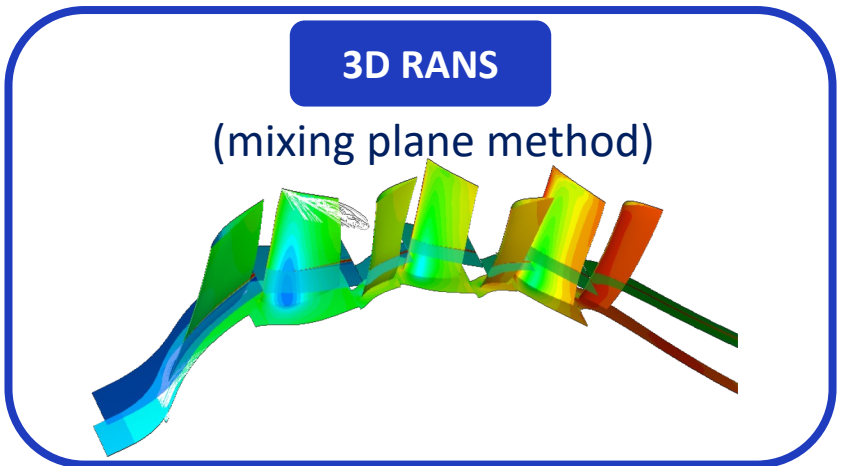
Modern high-loaded axial LP compressor



- Highly loaded
- High subsonic Mach number
- 3D modern blades



ASTEC



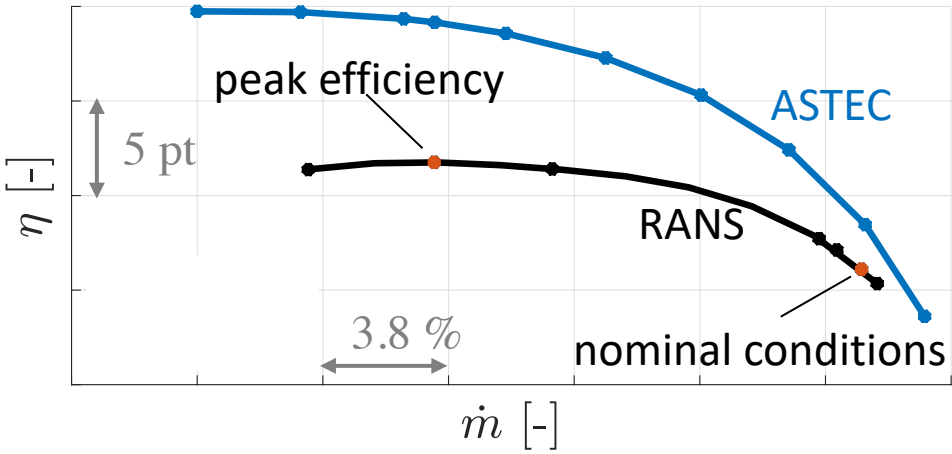
3D RANS

(mixing plane method)

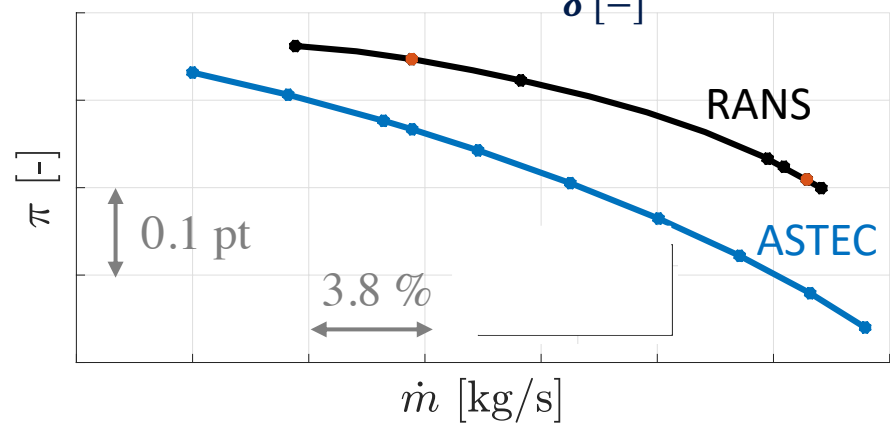
Modern compressor: comparison to RANS

- Low margin at nominal conditions
- More than 400 times faster (not yet optimized for speed)
- Increasing discrepancies near peak efficiency

Isentropic efficiency



Total pressure ratio



Correlations not calibrated for

- Optimized 3D blade geometries
- High subsonic Mach number



Closure model improvement

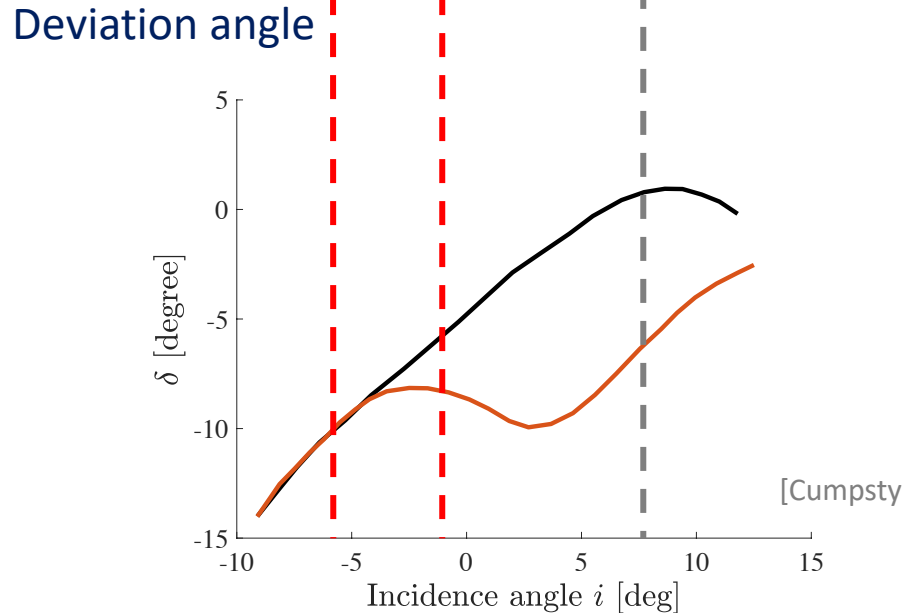
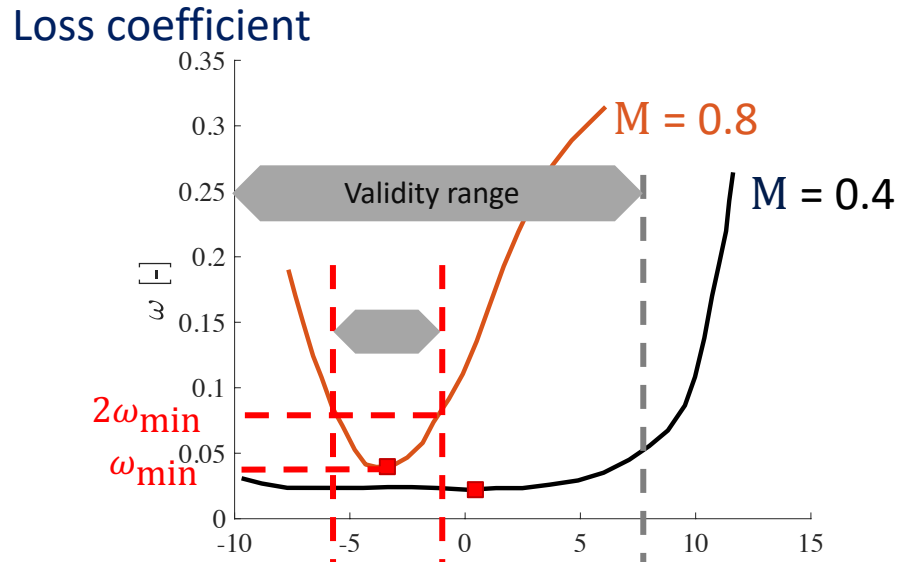
Modern compressor: comparison to RANS

Impact of Mach number

- Minimum-loss incidence angle shifted
- Increase of ω_{\min}
- Narrow range of validity
- Inconsistency between loss validity range and deviation linear range

Correlations **not calibrated** for these flow conditions

Measurements of C4-series cascade



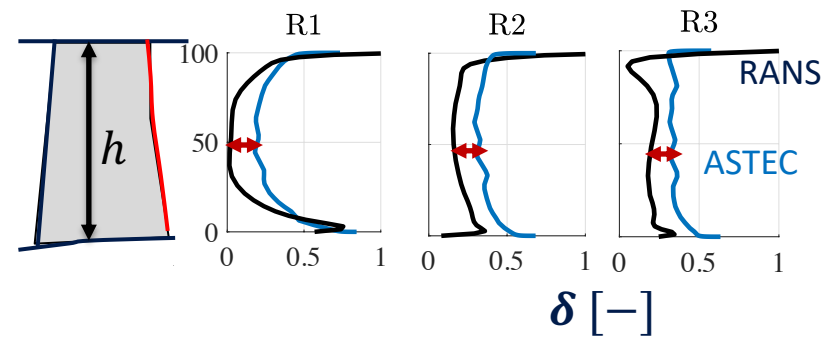
[Cumpsty 1989]

Modern compressor: comparison to RANS

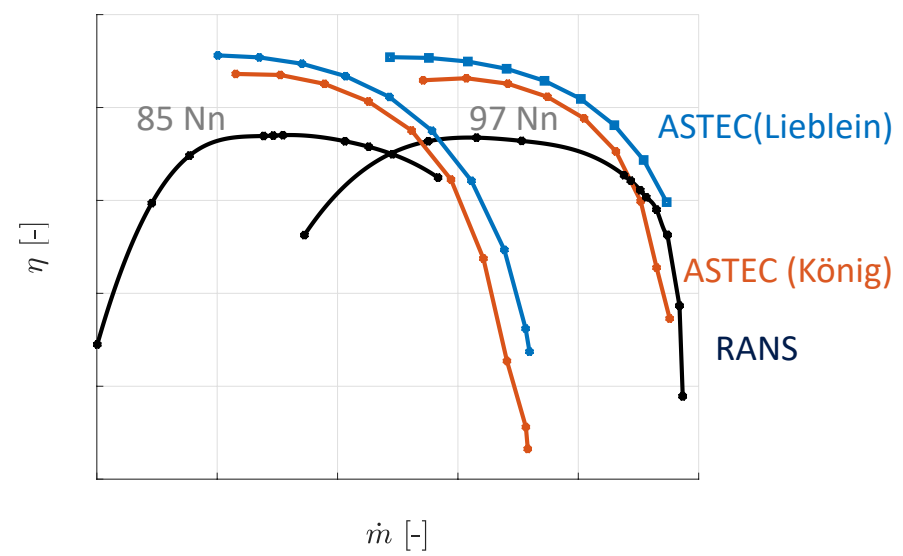
König's profile loss model (Bart Ruis' Master thesis)

- Mach number effect
- Valid beyond diffusion limit
- Compressibility

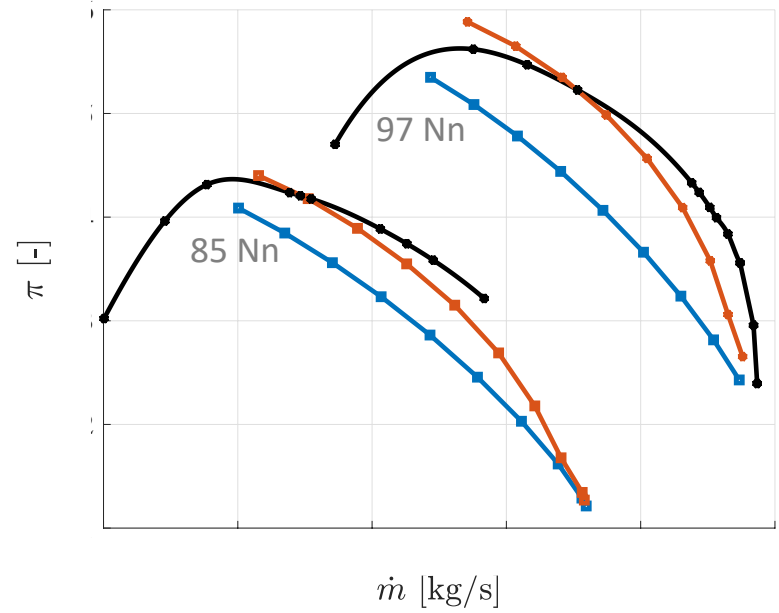
Correction for **Lieblein's** deviation angle:



Isentropic efficiency



Total pressure ratio



Conclusion

ASTE^C

- Closures computation: blade forces
- Coupled with **elsA**^[Onera]
→ **Navier-stokes** based through-flow model
- Correlations:
 - deviation angle
 - loss coefficient (profile loss)

Application to compressors

- Global good agreement for **CME2** compressor stage
- Improvement required for **modern axial-flow** compressor at high subsonic Mach
- Promising approach to drastically **reduce CPU cost** compared to 3D RANS

Outline

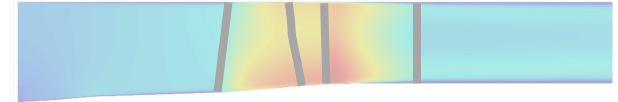
1

ASTECC: a viscous through-flow model

$$\frac{\partial U}{\partial t} + \frac{\partial(F-F_v)}{\partial x} + \frac{\partial(G-G_v)}{\partial r} = S$$

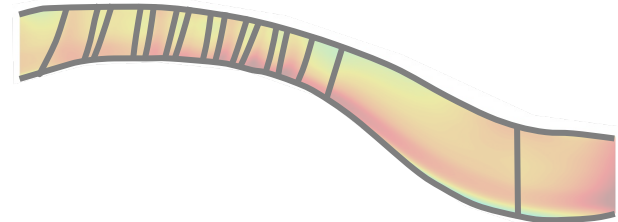
2

Application to the CME2 compressor stage



3

Application to an axial LP compressor



4

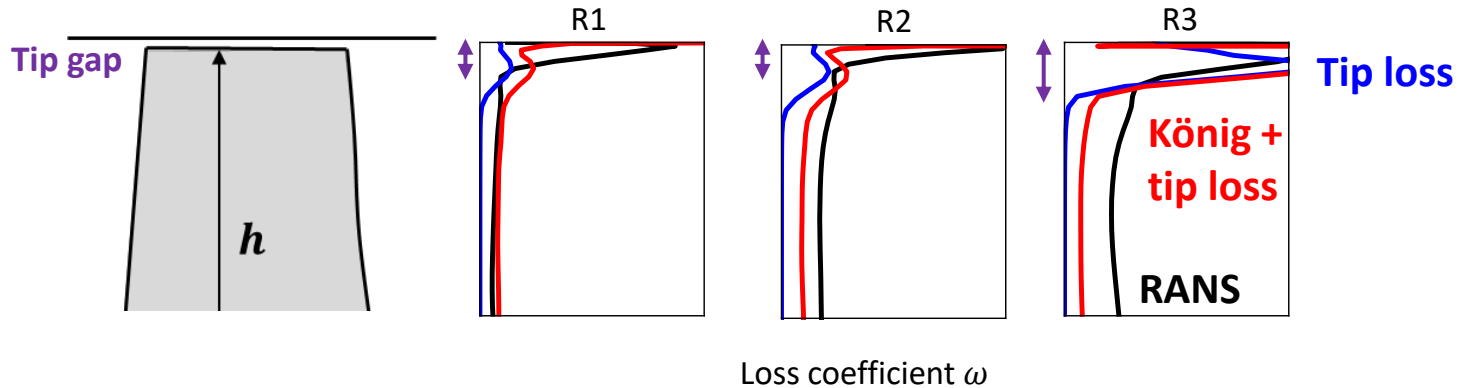
Future work



[SAB]

Future work: other sources of loss

- **Tip gap model: Lakshminarayana models**



- **Not efficient** for small tip gap (B.L. dominates loss production)
- **Endwall loss** partly taken into account by **NS model** but measurements used for correlations usually not performed close to endwalls ($\sim 5\%$ of blade height)

- **Secondary flows: in progress**

Corner vortex, horseshoe vortex, passage vortex
[Roberts, Ricci]

Future work: geometrical uncertainties

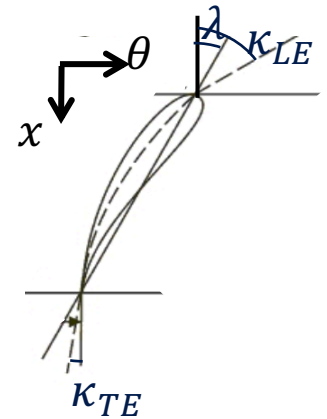
Parametric model

- Based on ASTEC's input parameters
- **Bounds based on SAB tolerances?**



No data from scanned blades

(Axisymmetric \rightarrow no mistuning as 3D steady computation)
 \rightarrow **Sensitivity analysis on performance and source terms**



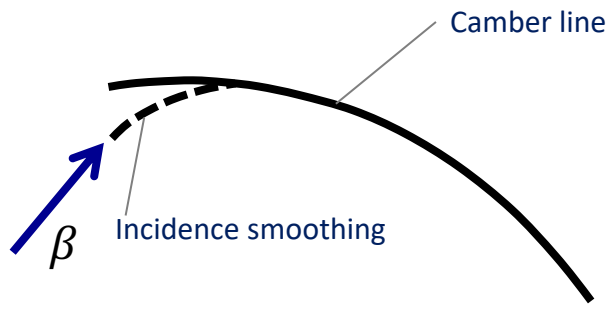
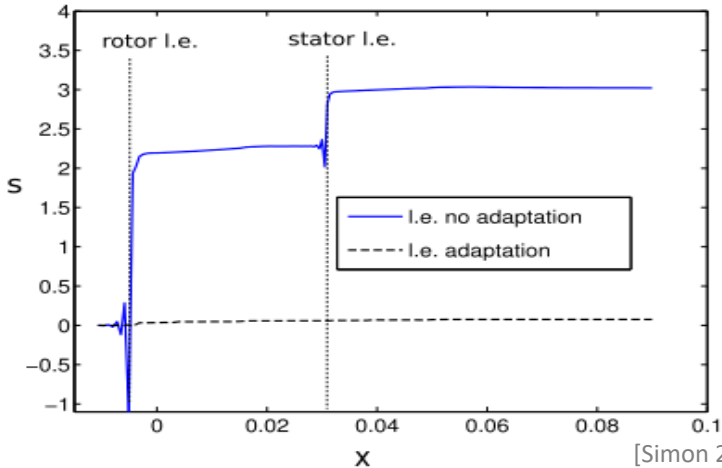
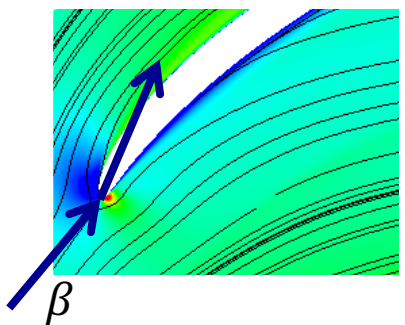
Uncertainties vs incidence correction

LE variabilities \rightarrow large impact on performance

But Axisymmetric model not able to predict flow prerotation at LE

\rightarrow Smoothing from upstream flow angle and flow angle imposed by models/blade geometry

\rightarrow Geometrical variabilities partially rubbed out



Acknowledgement

Funding for this research is provided by the Walloon region, under grant no. 7900, and Safran Aero Boosters in the frame of the project MARIETTA

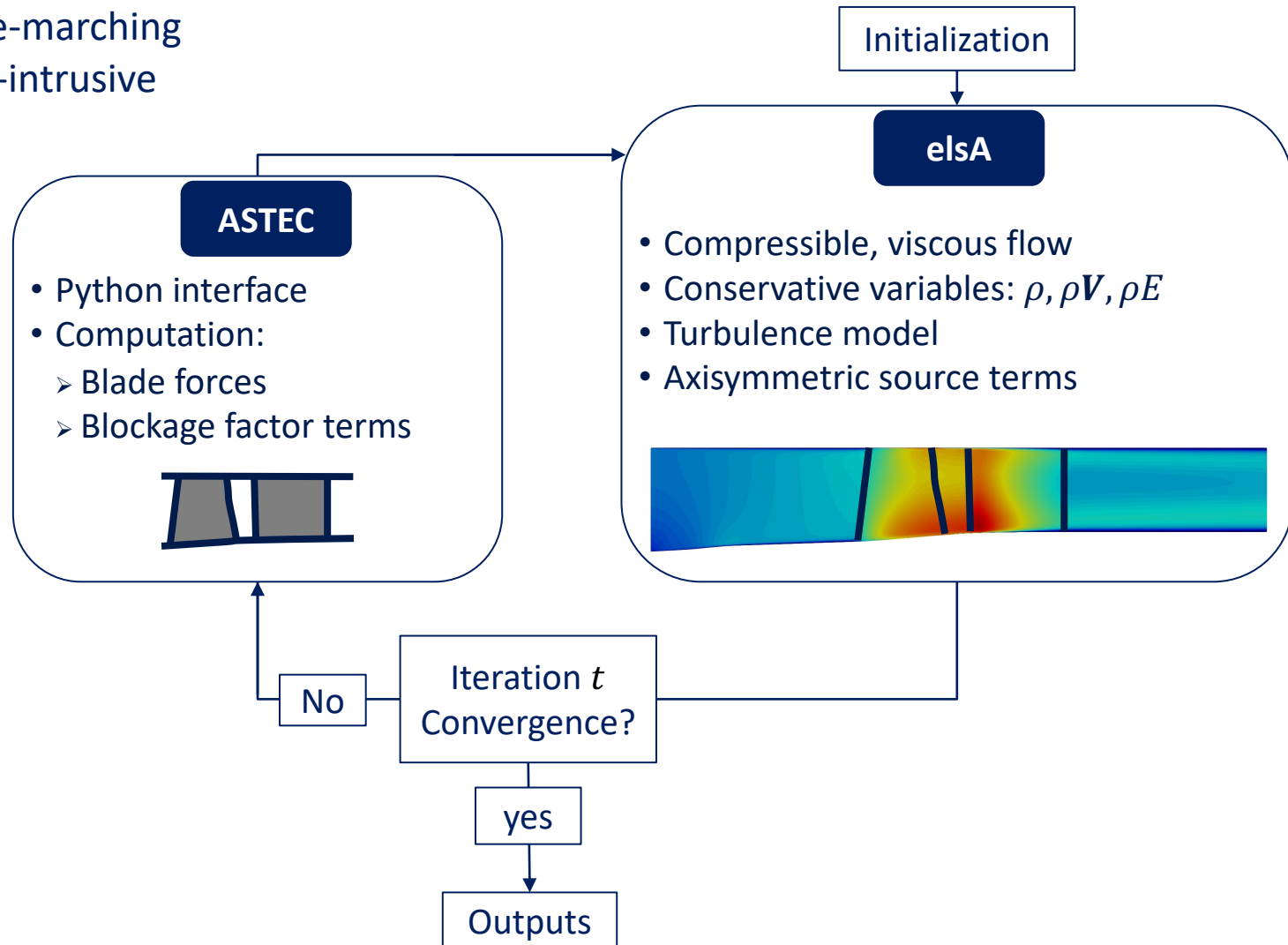


BACK-UP

Viscous through-flow model: ASTEC

Methodology:

- Time-marching
- Non-intrusive

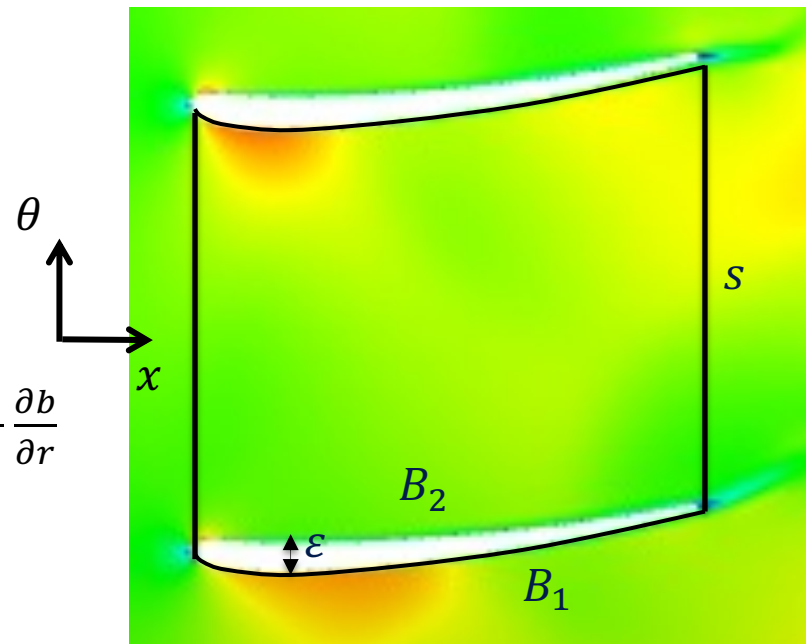


ASTECC: Inviscid blade force

Contributions: $\left\{ \begin{array}{l} \text{Blade blockage} \\ \text{Deflection force } \vec{f}_b \end{array} \right.$

- Streamtube contraction
- Known (averaged pressure p + geometry)
- Added to blockage factor terms

$$\mathbf{S}_{bi1} = \begin{bmatrix} 0 \\ \frac{p_{S1} + p_{S2}}{2b} \frac{\partial b}{\partial x} \\ \frac{p_{S1} + p_{S2}}{2b} \frac{\partial b}{\partial r} \\ 0 \\ 0 \end{bmatrix} \rightarrow \mathbf{S}_{bi1} = \begin{bmatrix} 0 \\ \frac{p}{b} \frac{\partial b}{\partial x} \\ \frac{p}{b} \frac{\partial b}{\partial r} \\ 0 \\ 0 \end{bmatrix} - \frac{F}{b} \frac{\partial b}{\partial x} - \frac{G}{b} \frac{\partial b}{\partial r}$$

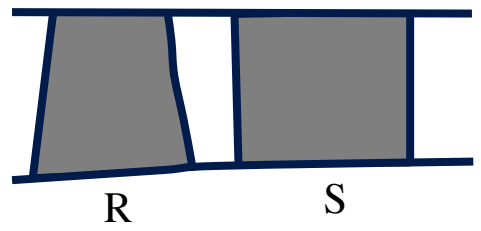


$$b = 1 - \frac{\varepsilon(x)}{s}$$

ASTEAC: inviscid blade force

Contributions: $\left\{ \begin{array}{l} \text{Blade blockage} \\ \text{Deflection force } \vec{f}_b \end{array} \right.$

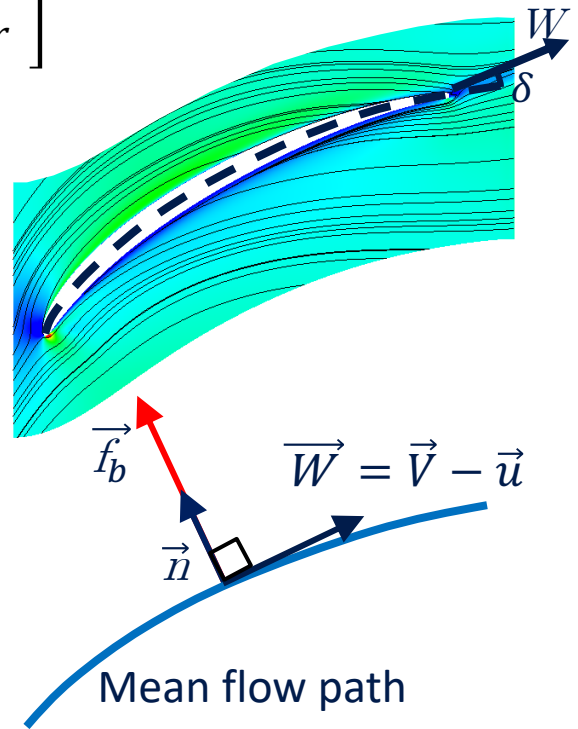
$$\mathbf{s}_{bi2} = \frac{N}{2\pi b} \begin{bmatrix} 0 \\ -[p]_{S1}^{S2} \frac{\partial \theta}{\partial x} \Big|_{cl} \\ -[p]_{S1}^{S2} \frac{\partial \theta}{\partial r} \Big|_{cl} \\ [p]_{S1}^{S2} \\ -[r]_{S1}^{S2} \Omega r \end{bmatrix} \rightarrow \mathbf{s}_{bi2} = \begin{bmatrix} 0 \\ f_{bx} \\ f_{br} \\ f_{b\theta} \\ f_{b\theta} \Omega r \end{bmatrix}$$



- Flow slips on the mean flow path (camber line + deviation angle δ)
- No entropy generation
- Iterative procedure:

$$\frac{\partial f_b}{\partial \tau} = -C(W_x n_x + W_r n_r + (W_\theta - \underbrace{\Omega r}_{u}) n_\theta)$$

[Simon 2007]

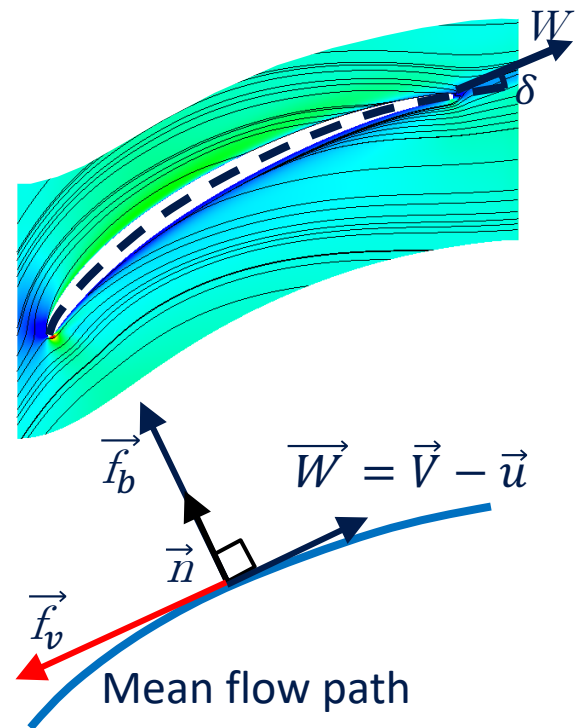
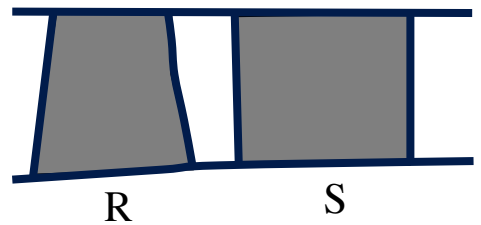


u : shaft rotation velocity
 V : velocity
 W : velocity in the relative frame
 Ω : shaft angular velocity

ASTECC: viscous blade force

- Distributed force \vec{f}_v

$$S_{bv} = \frac{N}{2\pi b} \begin{bmatrix} 0 \\ \left[\tau_{xj} \frac{\partial \theta}{\partial j} \right]_{S1}^{S2} \\ \left[\tau_{rj} \frac{\partial \theta}{\partial j} \right]_{S1}^{S2} \\ \left[\tau_{\theta j} \frac{\partial \theta}{\partial j} \right]_{S1}^{S2} \\ \left[\tau_{\theta j} \frac{\partial \theta}{\partial j} \right]_{S1}^{S2} \Omega r - \left[q_j \frac{\partial \theta}{\partial j} \right]_{S1}^{S2} \end{bmatrix} \rightarrow S_{bv} = \begin{bmatrix} 0 \\ f_{vx} \\ f_{vr} \\ f_{v\theta} \\ f_{v\theta} \Omega r \end{bmatrix}$$



- Entropy s generated:

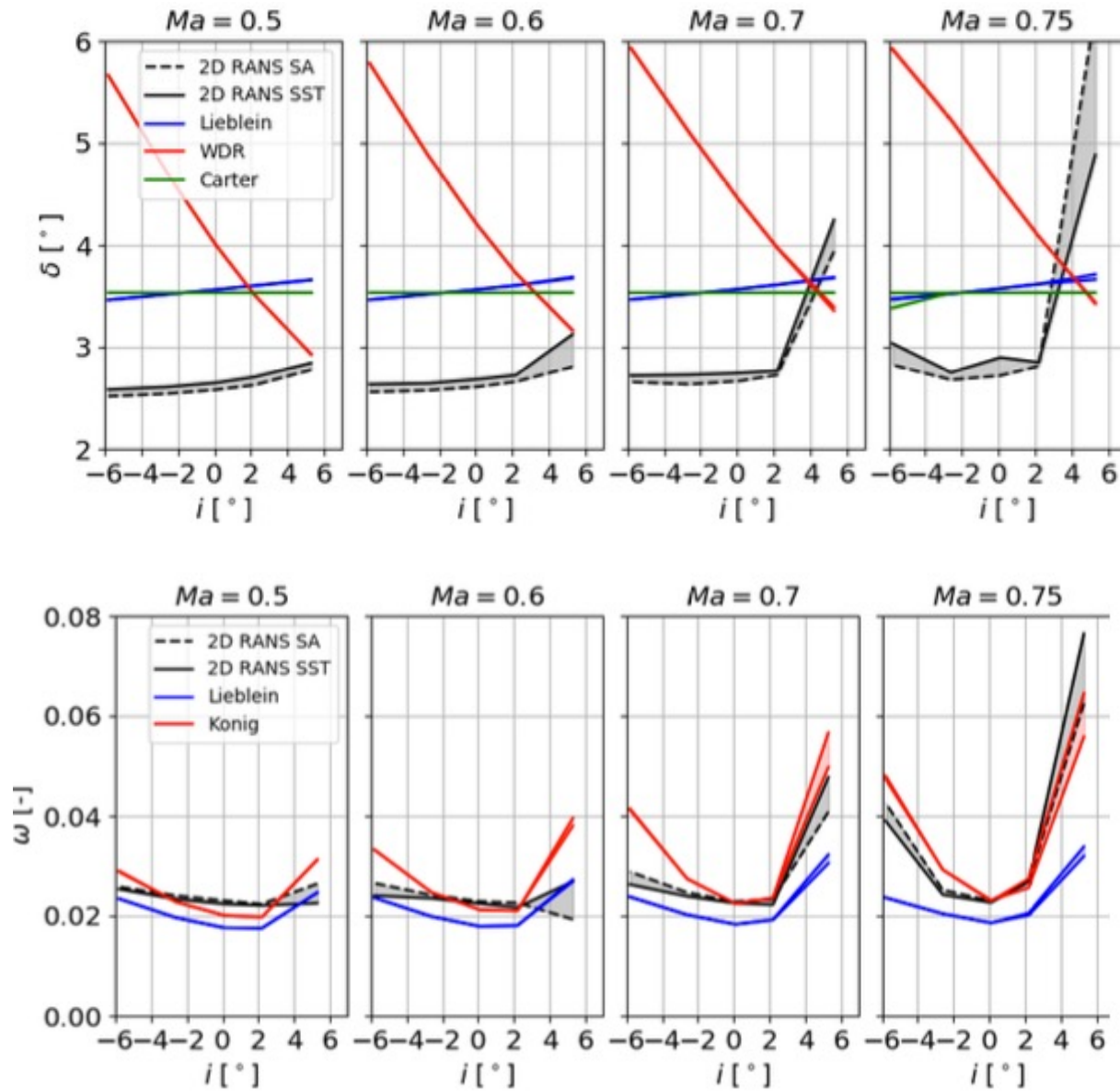
$$f_v = \rho T \frac{W_m \partial_m s}{W} = f(\omega) \quad \text{Loss coefficient}$$

[Hirsch 1988]

density temperature

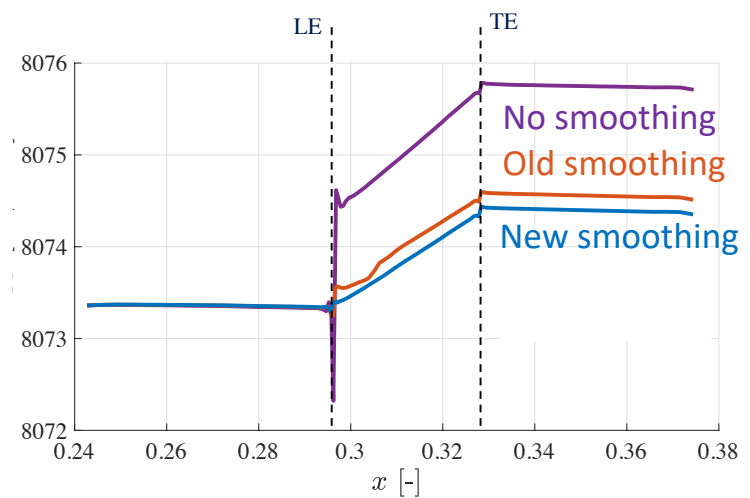
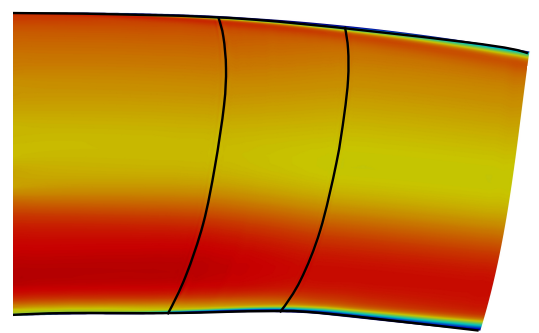
- ✓ Euler equations
- ~ N-S equations

Cascade computation (Bart Ruis)

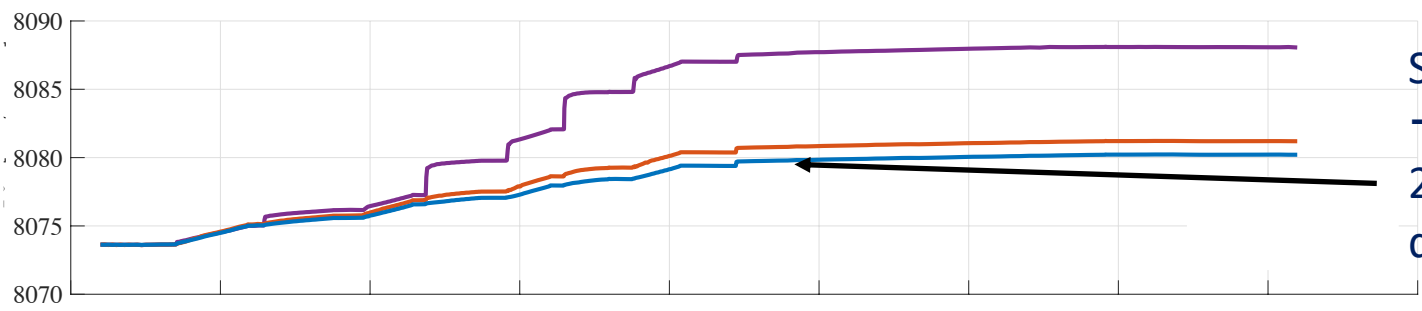


ASTECC: Mesh & incidence correction

Implementation of linear smoothing



New smoothing takes into account the deviation angle from correlations



Small peak
 → improvement:
 2nd order/ hyperbolic distribution

